Journal of Membrane Science Letters 3 (2023) 100065

Contents lists available at ScienceDirect

Journal of Membrane Science Letters

journal homepage: www.elsevier.com/locate/memlet

Strong improvement of permeability and rejection performance of graphene oxide membrane by engineered interlayer spacing

Zafar Khan Ghouri [a,b,*], Khaled Elsaid [c], David James Hughes [a], Mohamed Mahmoud Nasef [b,d], Ahmed Abdel-Wahab [c], Ahmed Abdala [c,1]

[a] School of Computing, Engineering and Digital Technologies, Teesside University, Middlesbrough TS1 3BX, Tees Valley, UK
[b] Center of Hydrogen Energy, Institute of Future Energy, Universiti Teknologi Malaysia, Jalan Sultan Yahya Petra, Kuala Lumpur 54100, Malaysia
[c] Chemical Engineering Program, Texas A&M University at Qatar, P.O. 23874, Doha, Qatar
[d] Malaysia-Japan International Institute of Technology, Universiti Teknologi Malaysia, Jalan Sultan Yahya Petra, Kuala Lumpur 54100, Malaysia

ARTICLE INFO

Keywords:
Graphene oxide
Amine groups
Functionalization
Water flux
Salt rejection

ABSTRACT

Advanced membranes fabricated from multilayer/laminated graphene oxide (GO) are promising in water treatment applications as they provide very high flux and excellent rejection of various water pollutants. However, these membranes have limited viability, and suffer from instabilities and swelling due to the hydrophilic nature of GO. In this work, the permeability and rejection performance of laminated GO membranes were improved via functionalization with ethylenediamine (EDA) and polyethyleneimine (PEI). The membranes are fabricated via the pressure-assembly stacking technique, and their structure is well characterized. The performance, rejection, and stability of the fabricated functionalized GO membranes were evaluated. Pillaring the GO layers using diamine and polyamine resulted in exceptionally high water permeability of 113 L/m^2h (LMH) compared to only 28 LMH for the pristine GO membrane while simultaneously satisfying high rejection of multivalent salts of 79.4, 35.4, and 19.6 % for Na_2SO_4, $MgCl_2$, and NaCl, respectively. The results obtained indicate that proper functionalization of GO provides a roadmap for the potential commercialization of such advanced membranes in water treatment applications.

Introduction

Seawater and brackish water desalination is the primary source of water for many countries, and more importantly, in the Arabian Gulf countries. On the other hand, the treatment of domestic and industrial wastewater can provide alternative water sources for industrial, agricultural, or landscaping applications. Moreover, wastewater associated with the oil, gas, and petrochemical industry, such as produced and process water, requires proper treatment to allow its reuse, reinjection into depleted oil and gas reservoirs, aquifer recharge, or sea disposal. Although the type and concentration of pollutants in produced and process water vary significantly based on their source, salts, and hydrocarbons are commonly present. Advanced treatment methods based on organic and inorganic membranes are gaining increased importance recently, yet these membranes suffer from fouling and permeability/selectivity trade-off.

In recent decades, two-dimensional (2D) nanomaterials exfoliated from layered compounds have gained significant research attention because of their outstanding physical and chemical properties for developing new and advanced membranes or enhancing the performance of commercial wastewater treatment membranes (Liu et al., 2015). Graphene and graphene oxide (GO), transition metal dichalcogenides (TMDs), graphitic carbon nitride (g-C_3N_4), MXene, metal-organic frameworks (MOFs), hexagonal boron nitride (h-BN) are typical classes of such 2D nanomaterials (Liu et al., 2018). Currently, graphene-based membranes are gaining more attention because of their outstanding mechanical properties, chemical-resistant nature, and atomic thickness (Shen et al., 2016; Huang et al., 2014). Graphene-based membranes can be categorized into three broad groups:

- Single- or few-layer graphene membranes with engineered Nano-sized pores (Cohen-Tanugi and Grossman, 2012; Surwade et al., 2016; Cohen-Tanugi and Grossman, 2014; Sun et al., 2015).

* Corresponding authors at: School of Computing, Engineering and Digital Technologies, Teesside University, Middlesbrough TS1 3BX, Tees Valley, UK.
E-mail addresses: Z.Ghouri@tees.ac.uk (Z.K. Ghouri), ahmed.abdala@qatar.tamu.edu (A. Abdala).
[1] Co-corresponding author.

https://doi.org/10.1016/j.memlet.2023.100065
Received 12 September 2023; Received in revised form 15 November 2023; Accepted 15 November 2023
Available online 24 November 2023

- Multilayers/laminated GO membrane (Dave et al., 2017; Hibbs et al., 2018; Hu and Mi, 2013).
- Membrane-based composites of graphene and its derivatives with different commercial membrane polymers (Hwang et al., 2016; Ganesh et al., 2013; Zinadini et al., 2014).

Multilayers or laminated GO on the substrate membranes can be easily formed by vacuum filtration, pressure assembly, and spray coating from GO solution (Chen et al., 2018). Nevertheless, multilayer/laminated GO membranes have some problems, such as the control of D-spacing between the GO laminates while reducing hydration in practical applications. The permeability and rejection behavior of the GO laminated membranes were mainly attributed to the transport channels formed by the D-spacing and the 'gap' between GO sheets in the laminated membrane (Zhang et al., 2019). The oxygen-containing functional groups such as hydroxyl, carbonyl, carboxyl, and epoxy on the basal plane and edge of GO could control the D-spacing in neighboring laminates and hydrophilicity of GO membranes (He et al., 1996). Monomeric and polymeric amines can be used for such purposes, as the functionalized amine group helps to tailor the D-spacing. Specifically, polyethyleneimine (PEI) is an organic water soluble polymer that contains primary, secondary, and tertiary amines groups (Kapilov-Buchman et al., 2015) not only has a great advantage for wastewater treatment (Li et al., 2018) but also is widely used for elimination of H_2S (Wang et al., 2007), CO_2 capturing (Drage et al., 2009), lipase immobilization (Khoobi et al., 2014) and gene transfection applications (Zheng et al., 2012). Recently, various engineered NF membranes have been developed for water filtration, such as PEI-mod-GO/PAA/PVA/GA/PAN (Wang et al., 2012), PEI/GO/PEI/-PAN (Nan et al., 2016), GO/PSf (Wei et al., 2016), TMPyP-GO/PES (Xu et al., 2016), GO—COOH/PSf (Yuan et al., 2017), brGO/PVDF (Han et al., 2013), GO/Nylon6 (Chen et al., 2018), GO/PSf (Hu and Mi, 2013), GO/PAN (Zhang et al., 2019). Therefore, to enhance the water permeability and multivalent ion rejection of fabricated membranes, ethylenediamine (EDA) and polyethyleneimine (PEI) were successfully grafted onto GO nanosheets to synthesize monomeric and polymeric amine-functionalized GO membrane, respectively. However, to characterize the structure and morphology of fabricated membranes, X-ray diffraction analysis (XRD), Raman spectroscopy, X-ray photoelectron spectroscopy (XPS), and scanning electron microscopy(SEM) were employed. The amine-functionalized GO was used to fabricate supported, and freestanding GO membranes, which have been evaluated for permeability, stability, and mono and multivalent ion rejection. In this way, the fabricated membranes could have enhanced water permeability (from 29 to 113 LMH) while satisfying high rejections (79.37 %, 35.43 %, and 19.6 % for Na_2SO_4, $MgCl_2$, and NaCl, respectively).

Results and discussions

Structure and morphology of GO, GO-EDA, and GO-PEI

The XRD characterizations were made to analyze the intercalation of amines into the interlayer spacing of GO. As shown in Fig. 1(A), the 2θ diffraction angle of GO-EDA and GO-PEI shifted significantly, suggesting that intercalation occurs due to the insetting of amine groups in GO during the functionalization. The corresponding D-spacing of pristine GO, GO-DEA, and GO-PEI was 0.91, 1.08, and 2.15 nm, respectively (Calculated by Bragg's equation $\lambda = 2d\text{Sin}\theta$, where λ is the wavelength in nm, d is the D-spacing in nm, and θ is the diffraction angle). The diffraction angle of pristine GO, GO-DEA, and GO-PEI are listed in SI (Table 1). The Raman spectra of pristine GO, GO-EDA, and GO-PEI powder are shown in Fig. 1(B). Pristine GO and amine-functionalized GO showed two distinct and broad peaks, the D band at around 1358 cm^{-1} and the G band at around 1590 cm^{-1}. Generally, the relative intensity ratio of D and G peaks (I_D/I_G) reflects the disordered (Sp^3) and ordered (Sp^2) carbon fractions (Aujara et al., 2019). It is noteworthy to mention that the intensity ratios of the D band to the G band of GO-EDA (0.94) and GO-PEI (0.95) were very close to that of pristine GO (0.92), which suggested that GO-EDA and GO-PEI retained the original skeleton structure of GO. The chemical compositions of pristine GO, GO-EDA, and GO-PEI powder were revealed by XPS, as shown in Fig. 1(C) the peaks at 284.8, 399.6, and 531.9 eV corresponded to C1s, N1s, and O1s, respectively. Notably, no N1s peak was observed in the survey spectrum of pristine GO. Nevertheless, the N1s peak appeared in the survey spectra of GO-EDA and GO-PEI. According to SI (Table 1), the oxygen atomic concentration dramatically decreased, while the carbon to oxygen ratio and nitrogen atomic concentration of GO-EDA and GO-PEI significantly increased. The N1s spectra of GO-EDA and GO-PEI (Fig. 1 (D and E)) show characteristic peaks of C—N and N—C═O at ~398.8 and ~399.9 eV, respectively (Zhang et al., 2018; YAN et al., 2012; Yan et al., 2013). The N1s spectra of GO-EDA (Fig. 1(D)) show a weakened peak of C—N compared to the N1s spectra of GO-PEI (Fig. 1(E). However, the XPS results further indicate that EDA and PEI molecules successfully grafted onto GO laminates via the formation of amide groups. The SEM image of the obtained GO powder is shown in SI (Fig. S3) where no noticeable changes in morphology can be seen between pristine GO (SI, Fig. S3(A)), GO-EDA (SI, Fig. S3(B)), and GO-PEI (SI, Fig.S3 (C)). It is clear that graphene oxide morphology was not changed by functionalization. The AFM image and corresponding height profile of GO are shown in SI, Fig.S4 indicating that the nanosheet has a lateral size of ~400 nm. In comparison, the prepared GO's thickness is approximately 0.45 nm without any visible defects, which is ideal for all types of filtration applications. The apparent GO thickness can correspond to a single-layer nanosheet, which is in good agreement with the theoretical thicknesses of single-layer GO (Medhekar et al., 2010).

The SEM images in Fig. 2(A–F) show the morphology of GO, GO-EDA and GO-PEI membrane sheets, which seem to be fully interconnected to membrane support and fully cover the pore of the support membrane without any structural defects (Fig. 2(A–C). In addition, the cross-sectional SEM images, Fig. 2(D–F) show that the GO sheet was stacked in the form of multilayers on the support, with approximate thicknesses of 1.0, 0.95 and 0.93 μm for pristine GO, GO-EDA and GO-PEI, respectively.

The surface topography of the GO, GO-EDA, and GO-PEI membranes was probed using AFM, as shown in SI (Fig.S5 (A-C)), and the measured surface roughness is provided in SI (Table S1). It can be seen, that the roughness of pristine GO and GO-EDA are quite similar, but surface roughness is increased by 54.8 % after functionalization with a polyamine (GO-PEI).

Regardless of the promising characteristics of GO membranes, they are not able to be commercialized due to their limited stability and durability associated with the swelling and delamination of the GO layers because water molecules enter the GO laminates and destroy hydrogen bonds and π-π interactions (Xia et al., 2015). Therefore, interlayer spacing is an important parameter determining membrane permeation characteristics (Cheng et al., 2016). Fig. 3 (A-C) shows the XRD patterns of synthesized membranes in both dry and wet states (all sets of membranes were soaked in distilled water for 1 h before XRD analysis). As shown in Fig. 3(A), 2θ of the pristine GO membrane significantly shifted from 9.7° at the dry state to 6.1° at the wet state. On the other hand, 2θ of the GO-EDA membrane was shifted only slightly (Fig. 3(B)). However, it is noteworthy to mention that the diffraction angle of the GO-PEI membrane is almost the same in both dry and wet conditions (Fig. 3(C)), indicating that GO-PEI showed similar interlayer spacing after swelling, which implies that water has a smaller influence on the interlayer spacing of GO-PEI/GO-EDA membranes than those of pristine GO membrane. This was probably due to the fact that intercalated amine molecules between GO laminates contribute to the resistance against swelling (Xia et al., 2015; Yang et al., 2013). The interlayer spacing of various membranes in their dry and wet conditions is shown in Fig. 3(D).

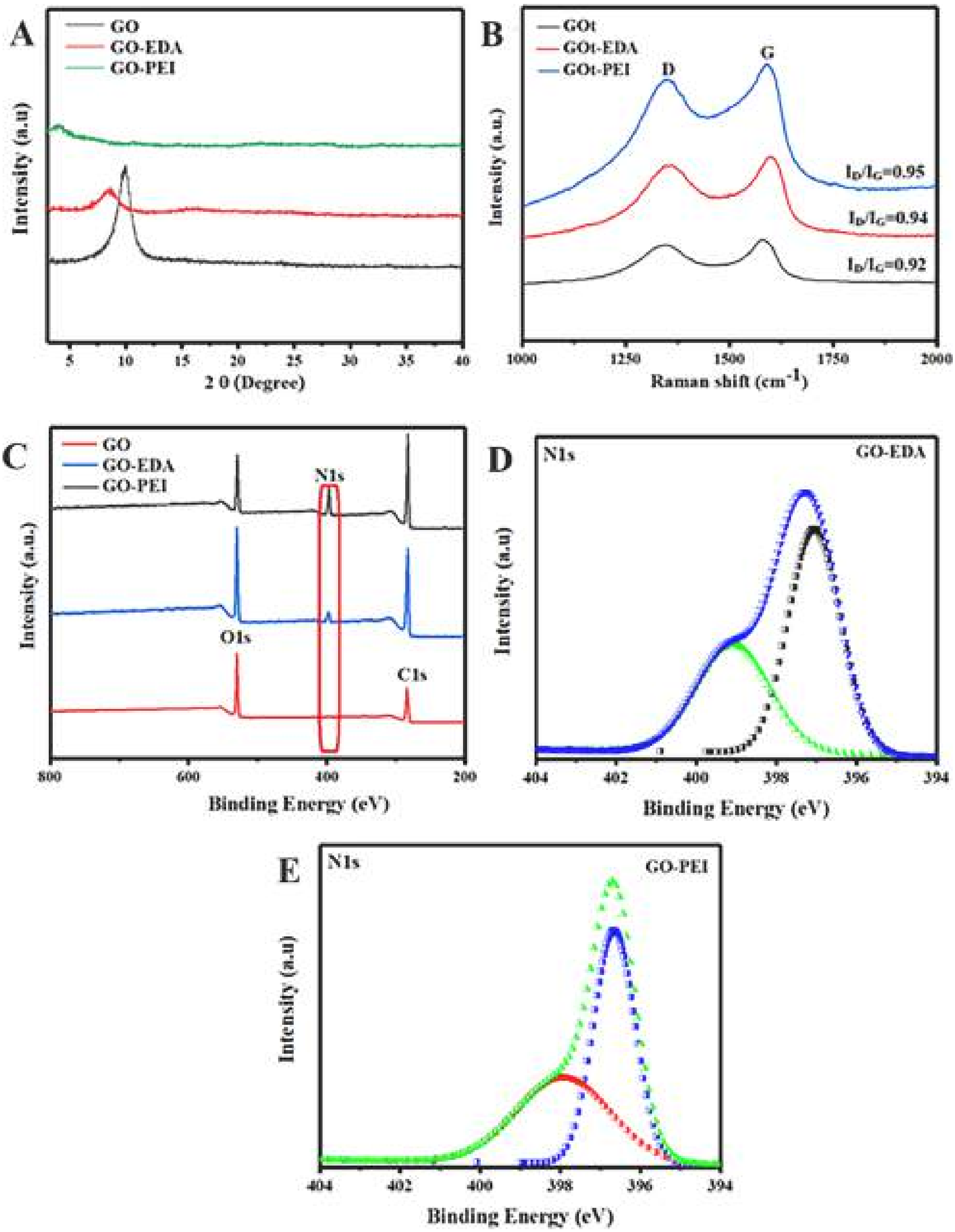

Fig 1. (A) XRD patterns, (B) Raman spectra of pristine GO, GO-EDA, and GO-PEI powder, (C) XPS full-scan spectra of pristine GO, GO-EDA, and GO-PEI powder, (D) N1s spectra of GO-EDA powder and (E) N1s spectra of GO-PEI powder.

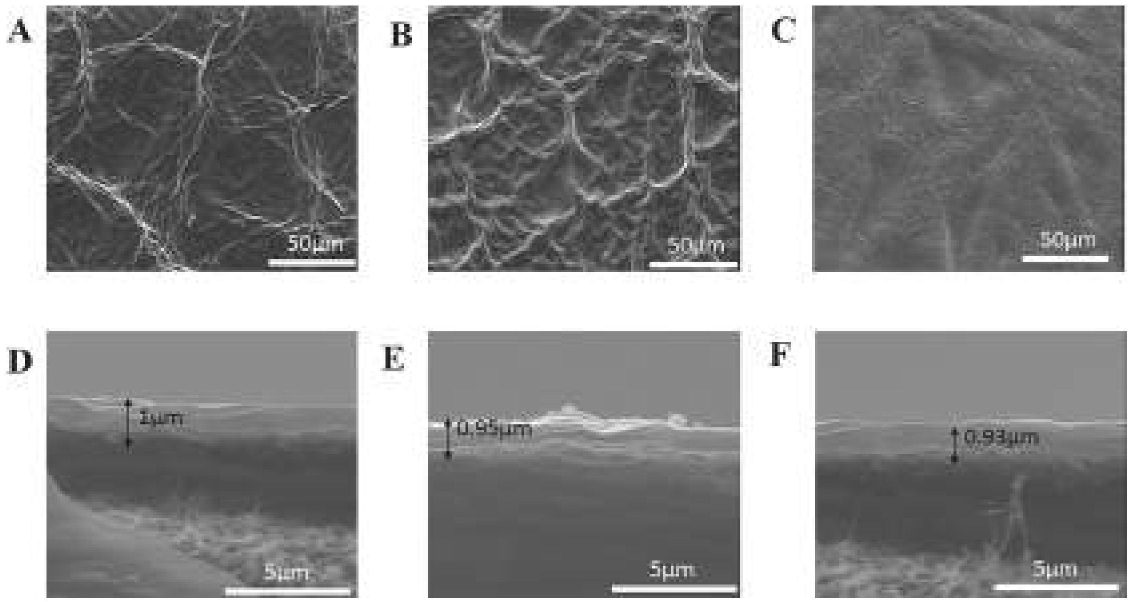

Fig 2. (A-C) top view and (D-F) cross-section SEM images of pristine GO, GO-EDA, and GO-PEI membranes, respectively.

Membrane performance assessment

Fig. 4(A) shows the water flux obtained with the GO, GO-DEA, and GO-PEI membranes. The GO membranes had the lowest flux of approximately 28 L/m^2h (LMH) due to their tight laminated structure. However, the pure water fluxes of the GO membranes were significantly affected by the amine functionalization. As can be seen, GO-DEA and GO-PEI membranes exhibited higher water fluxes corresponding to 59 and 113 LMH, respectively. Their water fluxes had increased by 103 and 289 % compared with that of the pristine GO membrane. This is translated into a pure water permanence (PWP) of 3.625, 7.375, and 14.125 LMHbar for pristine GO, GO-DEA, and GO-PEI, respectively.

To further assess the separation performance of pristine GO, GO-EDA and GO-PEI membranes toward salt ions, three common inorganic salts, i.e., NaCl, $MgCl_2$, and Na_2SO_4 were chosen as test salts with monovalent and divalent cations and anions. The rejections of the above salts by pristine and amine-functionalized GO membranes are displayed in Fig. 4 (B). The pristine GO membrane displayed a different salt rejection of 10, 16, and 57 % for NaCl, $MgCl_2$, and Na_2SO_4, respectively. In comparison with the pristine, monomeric amine-functionalized membrane (GO-DEA) demonstrated higher rejection performance with the same order NaCl $<$ $MgCl_2$ $<$ Na_2SO_4 of 16, 25, and 60 % for NaCl, $MgCl_2$, and Na_2SO_4, respectively. This is because divalent anions have higher electrostatic repulsion, steric hindrance, and lower diffusion coefficient similarly, the higher rejection of $MgCl_2$ compared to that of NaCl is understood by the large hydration radius and lower diffusion coefficient of Mg^{2+} ion relative to that of Na^+ (Zhang et al., 2019; Xia et al., 2015; Chen et al., 2017).

Similarly, the polymeric amine-functionalized membrane (GO-PEI) showed significantly improved rejection performance than the pristine GO and GO-EDA membranes. The GO-PEI membrane showed a 20, 35, and 80 % salt rejection performance for NaCl, $MgCl_2$, and Na_2SO_4, respectively.

The lowest salt rejection performance of pristine GO membrane can be ascribed to the severe swelling of GO laminate in wet conditions, which could allow salt ions to effortlessly migrate through the GO laminate. On the other hand, higher salt rejection of GO-PEI membrane can be attributed to the controlled D-spacing due to the insetting of amine groups into the GO laminates. Moreover, the insetting of amine groups into the GO laminates had an effect on membrane charge, explained by the Donnan exclusion concept, which leads to increased salt rejection. What's more, the introduction of nitrogen-containing groups (amine groups) in PEI contributes to the membrane more hydrophilicity due to interactions with water through H-bonding (Edokali et al., 2023)

Similar to the PW flux and PWP, SI, Table S2 shows that the membrane developed in this work has a comparable rejection to those of GO-modified UF membrane, with higher PWP.

Fig. 4(C) shows the normalized pure water (PW) and saline water flux of pristine GO, GO-EDA, and GO-PEI membranes over 12 hr test. The GO-PEI membrane maintained about 81–99 % of the initial rejection/flux, with higher stability retained for pure water permeation followed by that of NaCl, and the lowest for Na_2SO_4 over 12 h. A similar trend was observed for the GO-EDA membrane. In contrast, the pristine GO membrane retained only 86 and 72 % stability toward pure water and NaCl, which could be due to the membrane compaction under the applied pressure, hence reducing the membrane permanence. The stability test suggested that the D-spacing of modified membranes was higher than the D-spacing of the pristine one, which maintained the higher water flux over time, i.e. stability, by decreasing the membrane compaction effect.

Compared with the literature data on GO membrane (Zhang et al., 2019; Chen et al., 2017), the present work exhibited improved performance. This can be attributed to the fact that the small GO flakes (as observed by the AFM study (Fig.S4)) can facilitate abundant through-plane gaps allowing water molecules to enter the membrane, as flakes size is the predominant parameter governing the liquid permeation (Wang et al., 2016; Chong et al., 2018). Furthermore, single-layer GO can reduce the resistance to water permeation and the cross-linked amine can favor the formation of hydrated interlayer nanochannels and provide a strong hydrophilic surface, which contributed to significantly reducing the resistance to water permeation through the membrane, and correspondingly increasing the water flux. However, Table S2 provides some comparative values for the PWP of some GO-modified ultrafiltration (UF) membranes, along with their respective rejection to different salts. The table shows that the PWP for the membranes developed in this work have higher PWP than most reported GO-modified membranes.

Conclusion

This work demonstrated that the D-spacing of neighboring GO sheets

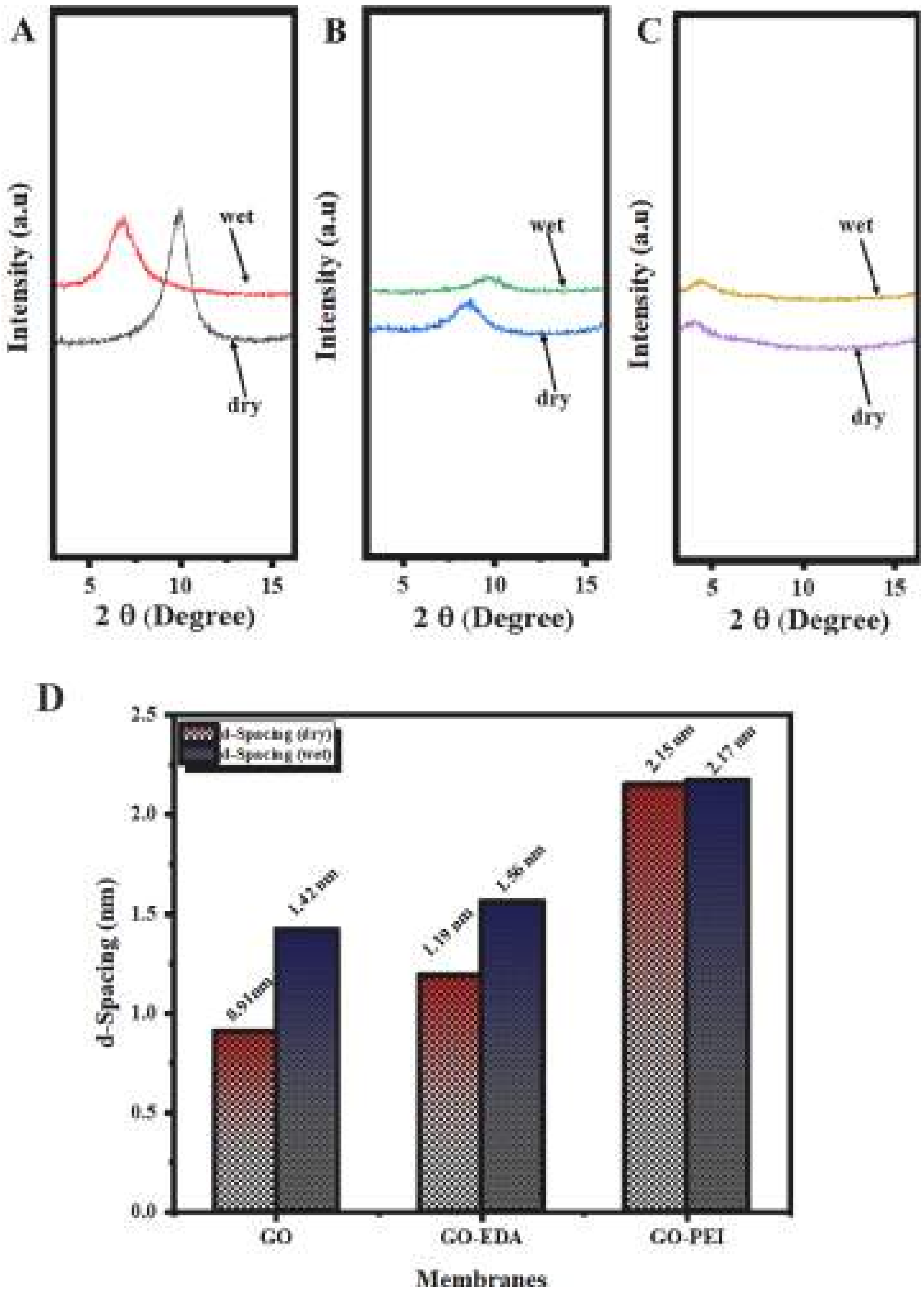

Fig 3. XRD patterns of (A) pristine GO, (B) GO-EDA, (C) GO-PEI membranes, and (D) corresponding d-spacing at day and wet sates, respectively.

could be tuned by simple chemical modification. Through grafting amine groups into the edge of the GO sheet, the interlayer spacing is expended which provides a wider molecule transport pathway and allows the water to permeate through laminated layers. Consequently, the fabricated membranes demonstrated enhanced water permanence (from 29 to 113 LMH) and satisfied high rejections (79.37 %, 35.43 %, and 19.6 % for Na_2SO_4, $MgCl_2$, and NaCl, respectively). Further, the presented results indicated that all fabricated membranes possessed excellent stability. This study demonstrated that the fabricated amine-functionalized GO membranes could be a promising candidate in wastewater treatment and desalination pretreatment for removing scale-forming constituents of divalent ions.

CRediT authorship contribution statement

Zafar Khan Ghouri: Methodology, Formal analysis, Validation, Funding acquisition, Writing – original draft. **Khaled Elsaid:** Validation, Formal analysis, Funding acquisition. **David James Hughes:** Writing – review & editing. **Mohamed Mahmoud Nasef:** Writing – review & editing. **Ahmed Abdel-Wahab:** Validation, Writing – review & editing. **Ahmed Abdala:** Conceptualization, Methodology, Validation, Funding acquisition, Writing – review & editing.

Declaration of Competing Interest

The authors declare no conflict of interest.

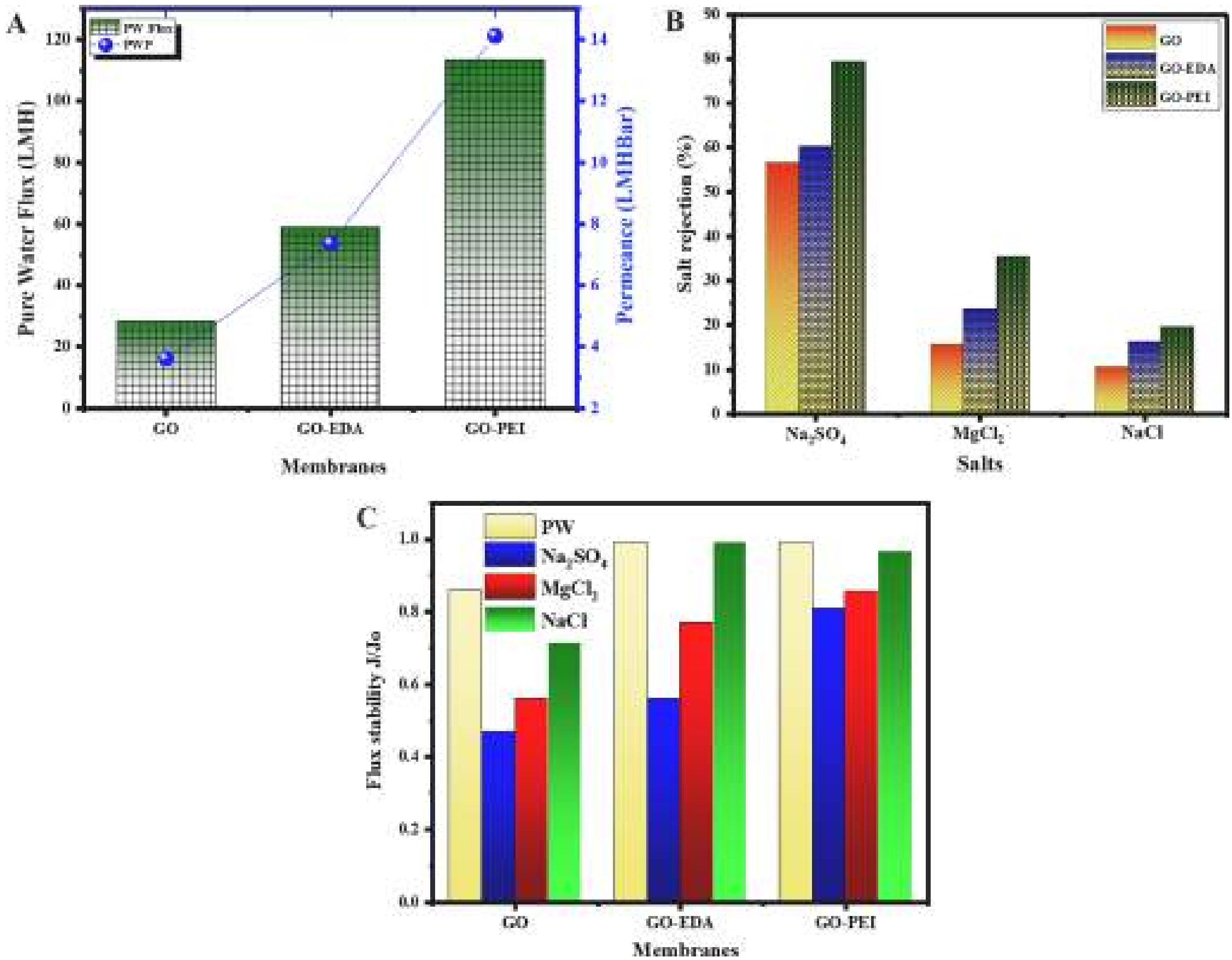

Fig 4. (A) Ph.-ure water flux, pure water permeance, (B) Salts rejection for pristine GO, GO-EDA, and GO-PEI membranes, and (C) Normalized flux stability for pristine GO, GO-EDA, and GO-PEI membranes after 12 h operation.

Data availability

Data will be made available on request.

Acknowledgements

We are grateful for the technical support from the Qatar Environment and Energy Research Institute QEERI. Further, Z.K.G and M.M.N wish to acknowledge Research Fellow Grant from Ministry of Higher Education through Universiti Teknologi Malaysia with Q. K130000.21A6.00P33.

Funding

This report was made possible by a UREP award [UREP23-056-2-028] from the Qatar National Research Fund (a member of The Qatar Foundation). The statements made herein are solely the responsibility of the author[*s*].

Supplementary materials

Supplementary material associated with this article can be found, in the online version, at doi:10.1016/j.memlet.2023.100065.

References

Aujara, K.M., Chieng, B.W., Ibrahim, N.A., Zainuddin, N., Thevy Ratnam, C., 2019. Gamma-Irradiation Induced Functionalization of Graphene Oxide with Organosilanes. Int J Mol Sci 20, 1910.

Chen, L., et al., 2017. Ion sieving in graphene oxide membranes via cationic control of interlayer spacing. Nature 550, 380–383.

Chen, L., et al., 2018. High performance graphene oxide nanofiltration membrane prepared by electrospraying for wastewater purification. Carbon N Y 130, 487–494.

Cheng, C., et al., 2016. Ion transport in complex layered graphene-based membranes with tuneable interlayer spacing. Sci Adv 2, e1501272. https://doi.org/10.1126/sciadv.1501272.

Chong, J.Y., Wang, B., Mattevi, C., Li, K., 2018. Dynamic microstructure of graphene oxide membranes and the permeation flux. J Memb. Sci. 549, 385–392. https://doi.org/10.1016/j.memsci.2017.12.018.

Cohen-Tanugi, D., Grossman, J.C., 2012. Water desalination across nanoporous graphene. Nano Lett. 12, 3602–3608.

Cohen-Tanugi, D., Grossman, J.C, 2014. Erratum: "Water permeability of nanoporous graphene at realistic pressures for reverse osmosis desalination"[J. C*hem.* P*hys.* 141, 074704 (2014)]. J. Chem. Phys. 141, 119901.

Dave, S.H., Keller, B., Han, G.D. & Grossman, J.C. (Google Patents, 2017).

Drage, T.C., Smith, K.M., Arenillas, A., Snape, C.E., 2009. Developing strategies for the regeneration of polyethylenimine based CO2 adsorbents. Energy Procedia 1, 875–880.

Edokali, M., et al., 2023. Chemical modification of reduced graphene oxide membranes: enhanced desalination performance and structural properties for forward osmosis. Chem. Eng. Res. Des. 199, 659–675. https://doi.org/10.1016/j.cherd.2023.10.022.

Ganesh, B., Isloor, A.M., Ismail, A.F., 2013. Enhanced hydrophilicity and salt rejection study of graphene oxide-polysulfone mixed matrix membrane. Desalination 313, 199–207.

Han, Y., Xu, Z., Gao, C., 2013. Ultrathin graphene nanofiltration membrane for water purification. Adv. Funct. Mater. 23, 3693–3700.

He, H., Riedl, T., Lerf, A., Klinowski, J., 1996. Solid-state NMR studies of the structure of graphite oxide. J Phys Chem 100, 19954–19958.

Hibbs, M. et al. Preparation and properties of graphene oxide/polymer desalination membranes. (Sandia National Lab.(SNL-NM), Albuquerque, NM (United States), 2018).

Hu, M., Mi, B., 2013. Enabling graphene oxide nanosheets as water separation membranes. Environ. Sci. Technol. 47, 3715–3723.

Huang, K., et al., 2014. A graphene oxide membrane with highly selective molecular separation of aqueous organic solution. Angew. Chem. 53, 6929–6932.

Hwang, T., et al., 2016. Ultrafiltration using graphene oxide surface-embedded polysulfone membranes. Sep. Purif. Technol. 166, 41–47.

Kapilov-Buchman, Y., Lellouche, E., Michaeli, S., Lellouche, J.-P., 2015. Unique surface modification of silica nanoparticles with polyethylenimine (PEI) for siRNA delivery using cerium cation coordination chemistry. Bioconjug. Chem. 26, 880–889.

Khoobi, M., et al., 2014. Synthesis of functionalized polyethylenimine-grafted mesoporous silica spheres and the effect of side arms on lipase immobilization and application. Biochem. Eng. J. 88, 131–141.

Li, K., et al., 2018. Fabrication of hierarchical MXene-based AuNPs-containing core–shell nanocomposites for high efficient catalysts. Green Energy Environ. 3, 147–155.

Liu, G., Jin, W., Xu, N., 2015. Graphene-based membranes. Chem. Soc. Rev. 44, 5016–5030.

Liu, G., et al., 2018. Ultrathin two-dimensional MXene membrane for pervaporation desalination. J. Memb. Sci. 548, 548–558.

Medhekar, N.V., Ramasubramaniam, A., Ruoff, R.S., Shenoy, V.B., 2010. Hydrogen bond networks in graphene oxide composite paper: structure and mechanical properties. ACS Nano 4, 2300–2306.

Nan, Q., Li, P., Cao, B., 2016. Fabrication of positively charged nanofiltration membrane via the layer-by-layer assembly of graphene oxide and polyethylenimine for desalination. Appl. Surf. Sci. 387, 521–528.

Shen, J., Zhang, M., Liu, G., Guan, K., Jin, W., 2016. Size effects of graphene oxide on mixed matrix membranes for CO2 separation. AIChE J. 62, 2843–2852.

Sun, C., Wen, B., Bai, B., 2015. Recent advances in nanoporous graphene membrane for gas separation and water purification. Sci. Bullet. 60, 1807–1823.

Surwade, S.P., et al., 2016. Corrigendum: water desalination using nanoporous single-layer graphene. Nat. Nanotechnol. 11, 995.

Wang, X., Ma, X., Sun, L., Song, C., 2007. A nanoporous polymeric sorbent for deep removal of H 2 S from gas mixtures for hydrogen purification. Green Chem. 9, 695–702.

Wang, N., Ji, S., Zhang, G., Li, J., Wang, L., 2012. Self-assembly of graphene oxide and polyelectrolyte complex nanohybrid membranes for nanofiltration and pervaporation. Chem. Eng. J. 213, 318–329.

Wang, S., et al., 2016. A highly permeable graphene oxide membrane with fast and selective transport nanochannels for efficient carbon capture. Energy Environ. Sci 9, 3107–3112. https://doi.org/10.1039/c6ee01984f.

Wei, Y., et al., 2016. Declining flux and narrowing nanochannels under wrinkles of compacted graphene oxide nanofiltration membranes. Carbon N Y 108, 568–575.

Xia, S., Ni, M., Zhu, T., Zhao, Y., Li, N., 2015. Ultrathin graphene oxide nanosheet membranes with various D-spacing assembled using the pressure-assisted filtration method for removing natural organic matter. Desalination 371, 78–87.

Xu, X.-L., et al., 2016. Graphene oxide nanofiltration membranes stabilized by cationic porphyrin for high salt rejection. ACS Appl. Mater. Interfaces 8, 12588–12593.

YAN, J.-l., et al., 2012. Functionalized graphene oxide with ethylenediamine and 1, 6-hexanediamine. New Carbon Mater. 27, 370–376.

Yan, J.-l., et al., 2013. Functionalized graphene oxide with ethylenediamine and 1, 6-hexanediamine. Carbon N Y 52, 624.

Yang, Y.H., Bolling, L., Priolo, M.A., Grunlan, J.C, 2013. Super gas barrier and selectivity of graphene oxide-polymer multilayer thin films. Adv. Mater. 25, 503–508.

Yuan, Y., et al., 2017. Enhanced desalination performance of carboxyl functionalized graphene oxide nanofiltration membranes. Desalination 405, 29–39.

Zhang, L., Chen, B., Ghaffar, A., Zhu, X., 2018. Nanocomposite membrane with polyethylenimine-grafted graphene oxide as a novel additive to enhance pollutant filtration performance. Environ. Sci. Technol. 52, 5920–5930.

Zhang, P., et al., 2019a. Enhanced permeability of rGO/S-GO layered membranes with tunable inter-structure for effective rejection of salts and dyes. Sep. Purif. Technol. 220, 309–319.

Zhang, M., Sun, J., Mao, Y., Liu, G., Jin, W., 2019b. Effect of substrate on formation and nanofiltration performance of graphene oxide membranes. J. Memb. Sci. 574, 196–204.

Zheng, M., et al., 2012. Poly (ethylene oxide) grafted with short polyethylenimine gives DNA polyplexes with superior colloidal stability, low cytotoxicity, and potent in vitro gene transfection under serum conditions. Biomacromolecules 13, 881–888.

Zinadini, S., Zinatizadeh, A.A., Rahimi, M., Vatanpour, V., Zangeneh, H., 2014. Preparation of a novel antifouling mixed matrix PES membrane by embedding graphene oxide nanoplates. J. Memb. Sci. 453, 292–301.